Available online at www.sciencedirect.com
SCIENCE DIRECT®
Journal of Power Sources 122 (2003) 153–161
JOURNAL OF POWER SOURCES
www.elsevier.com/locate/jpowsour

Preparation of negative electrodes for lithium-ion rechargeable battery by pressure-pulsed chemical vapor infiltration of pyrolytic carbon into electro-conductive forms

Yoshimi Ohzawa*, Masami Mitani, Takako Suzuki, Vinay Gupta, Tsuyoshi Nakajima

Department of Applied Chemistry, Aichi Institute of Technology, Yachigusa 1247, Yakusa-cho, Toyota 470-0392, Japan

Received 10 October 2002; received in revised form 13 February 2003; accepted 17 February 2003

Abstract

The plate-type negative electrodes for lithium-ion rechargeable battery were prepared by pressure-pulsed chemical vapor infiltration of pyrolytic carbon (pyrocarbon) into two sorts of conductive porous forms, that is, the carbonized paper (A) and the TiN-coated paper (B), as the conductive fillers and/or current collectors. The electrodes had the three-dimensionally continuous current paths in the pyrocarbon-based anodes without the organic binders and the additional conductive fillers. The pyrocarbon in sample (A) had the relatively high crystallinity, whereas the pyrocarbon in sample (B) was disordered. Sample (B) possessed higher surface area and larger pore volume with mesopores of 1.5–10 nm, especially below 3 nm, than that of sample (A). The capacity of pyrocarbon in sample (B) was 460 mA h g^{-1} per mass of pyrocarbon at a current density of 25 mA g^{-1}, reflecting the disordered microstructure of pyrocarbon film. And 80% of the capacity was maintained even at 1000 mA g^{-1}. The capacity of pyrocarbon in sample (A) was estimated at ~300 mA h g^{-1}, which was lower than that of sample (B). However, sample (A) showed higher Coulombic efficiency at first cycle (i.e. 85%) than that of sample (B), which would result from the high crystallinity, laminar microstructure and low surface area of pyrocarbon in sample (A).

Keywords: Chemical vapor deposition; Chemical vapor infiltration; Pyrolytic carbon; Lithium-ion battery

1. Introduction

The anode performance of lithium-ion battery strongly depends not only on the properties of carbon materials, but also the natures, the structures and the contents of organic binders and conductive fillers added to assist the construction of conduction network. In general, fine graphite or carbon black powders are utilized as the conductive fillers, however, the use of the fine particles leads to an increase in active surface area of electrode, resulting in the reactions with electrolytes. These reactions cause the irreversible loss and decline of capacity during charge–discharge cycling. Instead of the fine carbon particles, the use of fibrous conductive additives was examined. Micron-sized metal fibers with low active area and high conductivity are effective for enhancing the electrode capacity especially at a high rate with very low volumetric content [1]. Using of the vapor grown carbon fibers, the capacity and the cyclic life have been improved due to their excellent conductivity and high surface-to-volume ratio [2].

The chemical vapor infiltration (CVI) process was developed for matrix filling into fiber preforms to prepare the fiber-reinforced ceramics [3,4]. In last decade, three main methods were developed; isothermal and isobaric CVI (ICVI) [5,6], forced CVI (FCVI) [7,8] and pressure-pulsed CVI (PCVI). In the case of the continuous gas-flowed chemical vapor deposition (CVD) or ICVI, thick films were easily formed on external surface of the porous substrates or the particle-packed beds. Film formation on external surface prevented the source gas penetration into the substrates and the uniform coating throughout the substrates. In order to achieve the uniform coating on the conventional CVD, it is necessary to repeat the CVD treatment and the removal of films by polishing the external surface or the soft grind of particles at several times. On the other hand, the PCVI method consists of repetition of the following steps; evacuation of the reaction vessel, instantaneous introduction of the source gas, and holding to allow deposition [9–12]. This process allows homogeneous infiltration of matrix through the thickness of the preforms under suitable conditions

* Corresponding author. Tel.: +81-565-48-8121; fax: +81-565-48-0076.
E-mail address: ohzawa@ac.aitech.ac.jp (Y. Ohzawa).

0378-7753/03/$ – see front matter © 2003 Elsevier Science B.V. All rights reserved.
doi:10.1016/S0378-7753(03)00394-X

because of rapid penetration of the sources gas throughout the preform without pre-heating [13,14].

Using the PCVI method, porous SiC forms were prepared by partial densification with SiC matrix into the biologically derived porous preforms such as the carbonized wood, cotton and paper [15,16]. In similar process, highly porous electro-conductive forms would be obtained to partially infiltrate the electro-conductive materials such as TiN and TiC instead of SiC matrix. Utilizing these conductive porous forms as the conductive fillers and/or current collectors for lithium-ion rechargeable batteries, the negative electrodes containing the three-dimensionally continuous current paths would be prepared to infiltrate pyrolytic carbon (pyrocarbon) from the gas phase. Because the pyrocarbon films are directly deposited on the surface of current collector in the present process, it is expected that the contacting resistance between pyrocarbon and current collector is low even if no organic binder and additional conductive filler are used.

Pyrocarbon grown in CVD process shows the capacity of 250–700 mA h g^{-1} [17–21]. The electrochemical properties of pyrocarbon depend on macro-texture, microstructure, crystallinity and existence of foreign atoms, which can be varied by the CVD condition (e.g. temperature, pressure and hydrocarbon species) [18,22] and the source species for the dopants [19–21]. In addition to these factors, the sort of substrates on which pyrocarbon deposits would allow to affect the structure of pyrocarbon [17,23].

In this study, PCVI process was adopted to prepare the electrodes having the three-dimensionally continuous current paths by the infiltration of pyrocarbon into two sorts of conductive porous forms (the carbonized paper and the TiN-coated paper), and the relation between structure and electrochemical behavior of the infiltrated pyrocarbon was investigated.

2. Experimental

Fig. 1 shows the main part of the apparatus for PCVI. The source gas mixture was allowed to flow into a reservoir. It was instantaneously introduced (within 0.1 s) into the reaction vessel up to a pressure of 0.1 MPa, and the pressure was held under the same condition to allow matrix deposition for the desired time (holding time). Then, the gas was evacuated to below 0.7 kPa within 1.5 s. This cycle of the sequential steps was defined as one pulse, and it was repeated to the desired number of times.

Carbonized paper and TiN-coated paper were used as the highly porous conductive forms. The carbonized paper forms were prepared by the carbonization of commercial filter paper (ADVANTEC MFS) at 1000 °C in Ar for 4 h, and were cut to 10 mm × 15 mm × 0.5 mm. The TiN-coated paper forms were prepared by PCVI of TiN into the carbonized paper forms at 850 °C with holding time of 1.5 s from the gas system of $TiCl_4$ (1%)–N_2 (10%)–H_2. Pyrocarbon infiltration

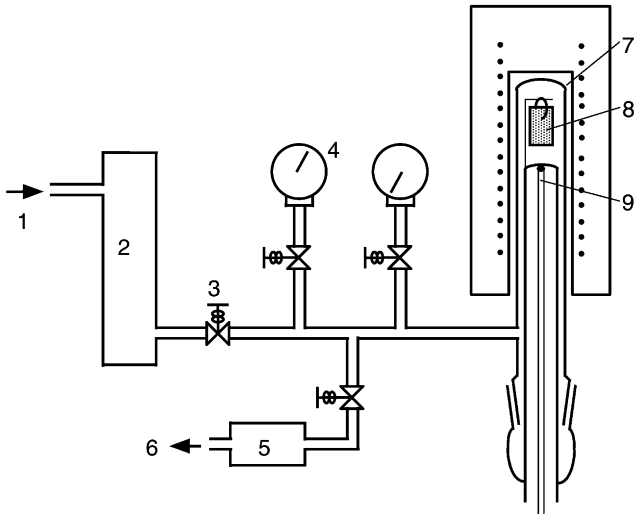

Fig. 1. Main part of apparatus for pressure-pulsed chemical vapor infiltration of pyrolytic carbon. (1) Source gas; (2) reservoir; (3) electromagnetic valve; (4) pressure gauge; (5) vacuum tank; (6) vacuum pump; (7) furnace; (8) substrates; (9) thermocouple.

into these porous forms was performed at 950 °C with holding time of 1.0 s using the gas system of C_3H_8 (30%)–H_2.

The average macropore size of the porous form was determined by the bubble-point method according to ASTM F 316, and geometric surface area was calculated from gas permeability using the Kozeny–Carman equation. Specific resistance was measured by four-terminal method.

The morphology of the samples was observed using scanning electron microscope (SEM, JEOL, JSM820). Structure of pyrocarbon was examined by X-ray diffraction (XRD) measurement (Shimazu, XD-610 with Cu Kα radiation) and Raman spectroscopy (Jasco, NRS1000 with Nd:YVO_4 laser of 532 nm). The Brunauer–Emmett–Teller (BET) surface area and mesopore volume distribution were measured using nitrogen gas (Micromeritics, Gemini 2375).

Galvanostatic charge–discharge cycling was made at 25 °C, using a three electrodes cell with metallic lithium as counter and reference electrodes in 1 mol l^{-1} $LiClO_4$ EC/DEC (1:1) solution. As-infiltrated samples were dried at 150 °C for 12 h under vacuum before using as working electrodes. The charge–discharge cycling was performed at an apparent current density of 0.2 mA cm^{-2} between 0 and 3 V versus Li/Li^+ unless particularly mentioned.

3. Results and discussion

3.1. Properties of conductive porous forms

Fig. 2 shows the SEM images of the carbonized paper forms {photographs (a) and (b)} and the TiN-coated paper forms {photographs (c) and (d)} prepared by 10,000 pulses of PCVI into the carbonized paper forms. From low-magnification photographs (a) and (c), it can be

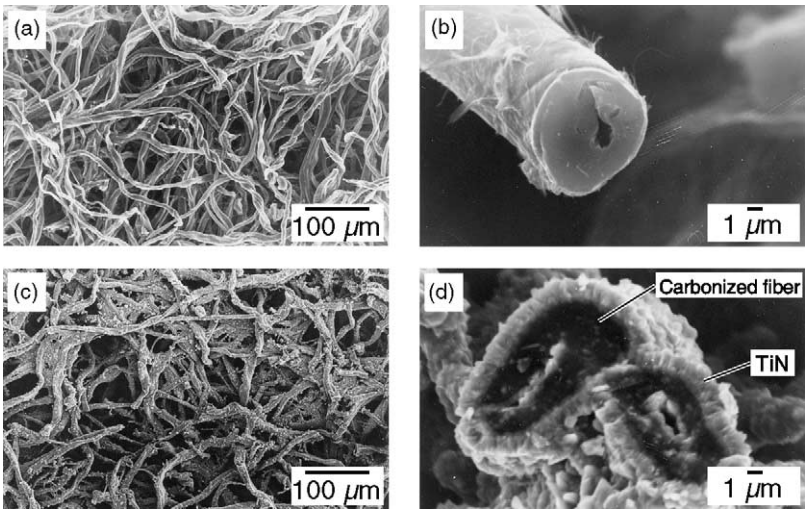

Fig. 2. SEM images of electro-conductive porous forms; (a) and (b) carbonized paper form, (c) and (d) TiN-coated paper form. TiN-coated paper form was prepared from carbonized paper form with 10,000 pulses in PCVI.

observed that the fibers have a relatively random orientation. Photographs (b) and (d) show high-magnification images of the cross-section of the forms (a) and (c), respectively. It can be found that TiN films with a thickness of 0.5–1 μm deposit around the carbonized fibers of about 6 μm in diameter. It appears that TiN films adhere tightly to the carbonized fibers, and the TiN-coated fibers connect with each other.

Table 1 shows the properties of carbonized paper and TiN-coated paper form as the current collector for the rechargeable batteries. Porosity of the carbonized paper form is in the range of 91–93%. Porosity of the TiN-coated paper form is lower than that of the carbonized paper form because of the partial infiltration of TiN. In the commercial lithium-ion battery, the volume fraction of the active materials layer per unit volume of the electrode was estimated to be about 75% from simple geometric calculation [24]. Porosity (i.e. free space for filling with active materials) of each form is higher than 75%. The apparent resistivity of TiN-coated paper form is below $10^{-5}\,\Omega\,m$, which is low enough for use as current collector. In the case of carbonized paper form, the resistivity shows relatively high value. Therefore, it is necessary to use it in combination with the conventional foil-type current collector. The average pore sizes of both forms are below 20 μm, which are lower than the thickness of the active materials layer in the commercial lithium-ion battery and the pore size of the metal (Ni) foam current collector for Ni–Cd battery. Large cavity is unsuitable because of the low conductivity of the active materials and the electrolytes for lithium-ion rechargeable battery. The geometric surface area per unit volume showed higher value than that of the conventional current collector. Therefore, it is expected that contacting resistance between active materials and current collector is reduced when the present forms are used as current collector. The carbonized paper form has the capacity of around $300\,mA\,h\,g^{-1}$. This form could act as not only the current collector but also the host material for lithium intercalation/de-intercalation. On the other hand, the capacity of TiN-coated form is extremely low ($<10\,mA\,h\,g^{-1}$). It is considered that TiN is inert against the electrochemical reaction with lithium-ion under the present condition.

3.2. Structures of pyrocarbons infiltrated into conductive porous forms

Pyrocarbon was infiltrated into the carbonized paper and TiN-coated forms at 950 °C with holding time of 1 s from gas system of C_3H_8 (30%)–H_2. Fig. 3 shows the relation between the number of pulses and the filling ratio of pyrocarbon, which is defined as the fraction of infiltrated pyrocarbon volume per initial pore volume in the forms. The filling ratio increases almost linearly, and infiltration rates for both forms are close to each other. The filling ratio after 50,000 pulses is 70%, which corresponds to the residual porosity of

Table 1
Specific properties of carbonized paper form and TiN-coated paper form

Form	Porosity (%)	Resistivity (Ω m)	Average pore size (μm)	Geometric surface area ($m^2\,m^{-3}$)	Charge capacity[a] ($mA\,hg^{-1}$)
Carbonized paper	91–93	4×10^{-3}	19	$7–9 \times 10^4$	280–320
TiN-coated paper[b]	84–88	9×10^{-6}	18	$8–10 \times 10^4$	10

[a] Measured at current density of $0.2\,mA\,cm^{-1}$.
[b] Number of pulses in PCVI treatment; 10,000.

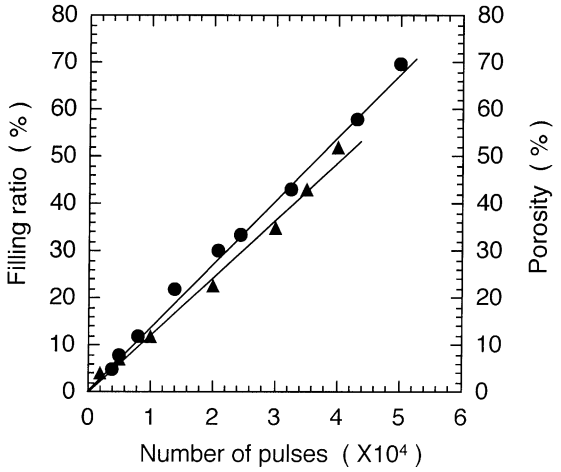

Fig. 3. Relation between number of pulses and filling ratio of pyrolytic carbon into carbonized paper form (▲) and TiN-coated paper form (●).

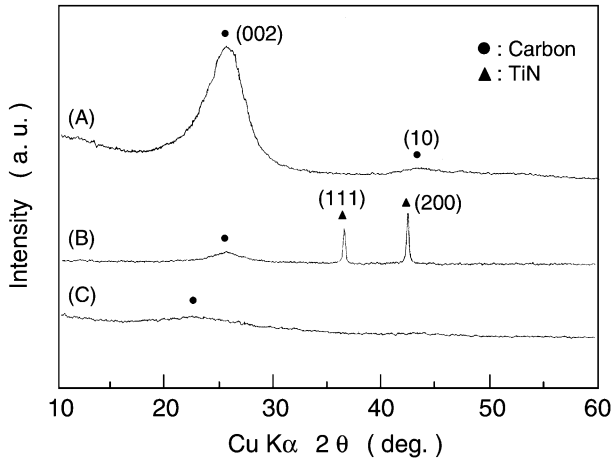

Fig. 5. X-ray diffraction patterns from the external surface of carbonized paper/pyrolytic carbon sample (A), carbonized paper/TiN/pyrolytic carbon sample (B) and original carbonized paper form (C). Number of pulses in PCVI for pyrolytic carbon, 25,000.

28%. Further infiltration causes the film formation on an external surface of the porous form, which would prevent the in-depth penetration of the electrolyte into the electrode. For the sample obtained after 40,000 pulses of PCVI, mass fraction of pyrocarbon per unit volume of the electrode reaches to 0.9 g cm^{-3}, which is in the similar range with that of the electrode for the commercial lithium-ion battery [25].

Fig. 4 shows the SEM images of the carbonized paper/pyrocarbon samples {photographs (a) and (b)} and the carbonized paper/TiN/pyrocarbon samples {photographs (c) and (d)}. From low-magnification micrographs (a) and (c), it can be observed that the fibers have a relatively random orientation and connect with each other. From the images (b) and (d), it can be found that the dense films of pyrocarbon with a thickness of ~3 μm are formed on the carbonized fibers and the TiN films, respectively. The pyrocarbon films were almost uniform in thickness throughout the preforms. These SEM observations indicate that three-dimensional current paths having a relatively random orientation are formed in the active material layers of the negative electrodes. In micrographs (b) and (d), it appears that pyrocarbon films adhere tightly to carbonized fiber or TiN. From these results, it is expected that the contacting resistance between active material (pyrocarbon) and current collector is relatively low even if no organic binders and additional conductive fillers are used. It is found that pyrocarbon has the laminar texture oriented parallel to the surface of the carbonized fiber. The laminar structure appears remarkably in pyrocarbon deposited directly on the carbonized fiber as shown in photograph (b).

Fig. 5 shows the X-ray diffraction (XRD) patterns of the samples (A) and (B) infiltrated with pyrocarbon and the original carbonized paper form (C). The filling ratios of pyrocarbon in the samples (A) and (B) are 45 and 48%, respectively.

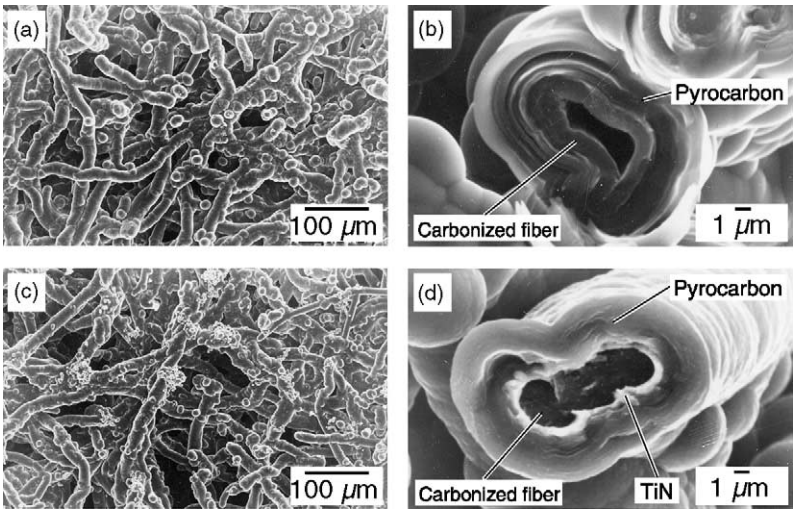

Fig. 4. SEM images of carbonized paper/pyrolytic carbon {(a) and (b)} and carbonized paper/TiN/pyrolytic carbon {(c) and (d)} samples. Number of pulses in PCVI for pyrolytic carbon; (a) and (b) 35,000, (c) and (d) 32,500.

For the original form (C), it can be observed that (0 0 2) diffraction peak at 2θ of 22.7° (d_{002} = 3.99 nm) is very weak and broad, reflecting the low crystallinity of carbon obtained from the carbonization of cellulose fiber. However, for carbonized paper/pyrocarbon sample (A), a strong (0 0 2) peak appears at higher angle of 25.4° (d_{002} = 3.59 nm). These results indicate that the crystallinity of pyrocarbon deposited on carbonized fiber is much higher than that of the substrate carbon. On the other hand, the intensity of (0 0 2) diffraction line for carbonized paper/TiN/pyrocarbon sample (B) is significantly weak though the filling ratio of pyrocarbon is similar in both samples, and the peak position of (0 0 2) line for sample (B) is close to that for sample (A). As shown in Fig. 4 {SEM image (b)}, pyrocarbon in sample (A) has the laminar texture parallel to the surface of the carbonized fiber in paper preform. This orientation may result in the strong intensity of (0 0 2) diffraction line of sample (A). On the other hand, it is suggested that the orientation in pyrocarbon deposited on TiN-coated fiber in sample (B) is disturbed, i.e. the degree of structural disordering in pyrocarbon of sample (B) is high compared with pyrocarbon of sample (A).

Fig. 6 shows the Raman spectra of the carbonized paper form (C), the carbonized paper/pyrocarbon (A) and the carbonized paper/TiN/pyrocarbon (B) samples. Two peaks are observed at about 1580 and 1360 cm^{-1} for each sample. The peak observed at 1580 cm^{-1} indicates E_{2g2} vibration mode derived from graphitic structure of carbon materials (G-band), whereas the peak at 1360 cm^{-1} indicates A_{1g} mode arising from the disordered structure and/or edge of carbon particles (D-band) [26,27]. The peak intensity of D-band for the original form (C) is strong compared with that for pyrocarbon in sample (A) or (B). The difference in D-band intensity results from higher crystallinity of pyrocarbon than that of carbonized fiber, which is confirmed by XRD measurement as shown in Fig. 5. The intensity ratio of two peaks, R value (I_D/I_G), is calculated to represent the degree of surface disordering of pyrocarbon film. In Fig. 7, R values are plotted as a function of pulse number in PCVI treatment. R values for both samples (A) and (B) slightly decrease with number of pulses. However, R value for sample (B) is somewhat higher than that for sample (A) on each stage of PCVI treatment. This result indicates that the degree of structural disordering in pyrocarbon deposited on TiN-coated fiber {sample (B)} is high in comparison with pyrocarbon directly deposited on carbonized fiber {sample (A)}.

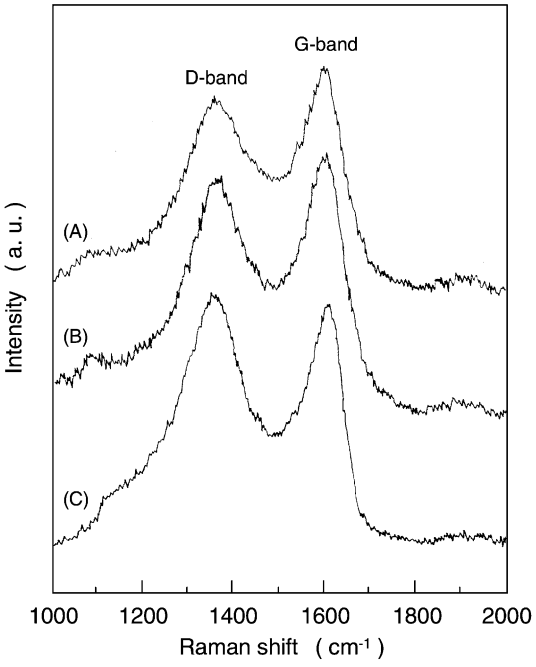

Fig. 6. Raman spectra of carbonized paper/pyrolytic carbon sample (A), carbonized paper/TiN/pyrolytic carbon sample (B) and original carbonized paper form (C). Number of pulses in PCVI for pyrolytic carbon, 5000.

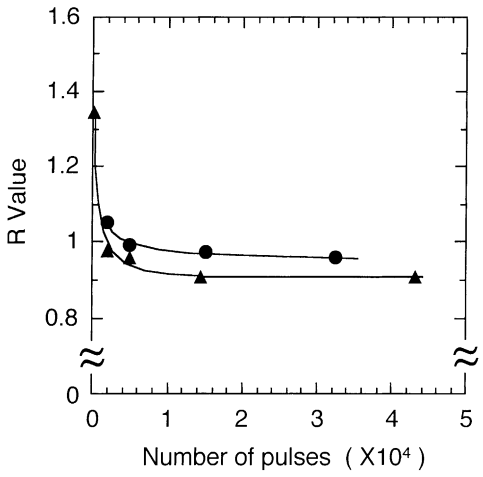

Fig. 7. R values (I_D/I_G) of carbonized paper/pyrolytic carbon sample (▲) and carbonized paper/TiN/pyrolytic carbon sample (●) as a function of number of pulses.

In the case of the continuous gas-flowed CVD, the source gases are pre-heated before reaching the surface of substrate to lead the formation of active precursors followed by the nucleation, which often causes the formation of the high molecular weight compounds such as tar or the carbon soot. Co-deposition of tar or soot would affect the crystallinity of pyrocarbon film. In PCVI process, instantaneous introduction of the source gas and evacuation of the reacted gas are repeated at relatively short intervals. As the sources gas rapidly penetrates throughout the preform without pre-heating, nucleation in gas phase is restrained, and crystal growth is promoted in evacuation step. These may result in the relatively high crystallinity of pyrocarbon in sample (A). However, the degree of structural disordering in pyrocarbon deposited on TiN-coated fiber {sample (B)} is high in comparison with pyrocarbon directly deposited on carbonized fiber {sample (A)}. It is supposed that the formation of C–C bonds between pyrocarbon and substrate carbon for sample (A) is easier than that for

Table 2
BET surface area data of original carbonized paper form, carbonized paper/pyrolytic carbon sample (A) and carbonized paper/TiN/pyrolytic carbon sample (B)

Sample	BET surface area ($m^2\ g^{-1}$)
Original carbonized paper form	170–210
(A) Carbonized paper/pyrolytic carbon[a]	0.81
(B) Carbonized paper/TiN/pyrolytic carbon[a]	33

[a] Number of pulses in PCVI treatment for pyrolytic carbon; 5000.

sample (B), which may affect the crystal growth rate on the surface of substrate. In addition, Ti atoms easily react with carbon to form TiC. This may cause the difference of microstructure of pyrocarbon in each sample. However, the detail of growth mechanism is now open to further investigation.

In Table 2, the surface area data obtained by BET method are shown for the carbonized paper/pyrocarbon sample (A), the carbonized paper/TiN/pyrocarbon sample (B) and the original carbonized paper form. The surface area of original form decreases from 210 to 0.81 $m^2\ g^{-1}$ by the infiltration of pyrocarbon. This result indicates that the dense pyrocarbon film covers the almost all surface of porous carbonized fiber. The surface area of sample (B) is higher than that of sample (A). It is supposed that pyrocarbon deposited on TiN in sample (B) is porous in nanometer size, as compared with pyrocarbon deposited directly on carbonized fiber in sample (A). Pore volume distribution data of both samples are shown in Fig. 8. It is found that sample (B) has the mesopores with diameter of 1.5–10 nm, and the volume fraction of mesopores below 3 nm is extremely large. It is expected that these mesopores below 3 nm may accommodate some amount of excess lithium in addition to lithium insertion into the interlayer of graphite.

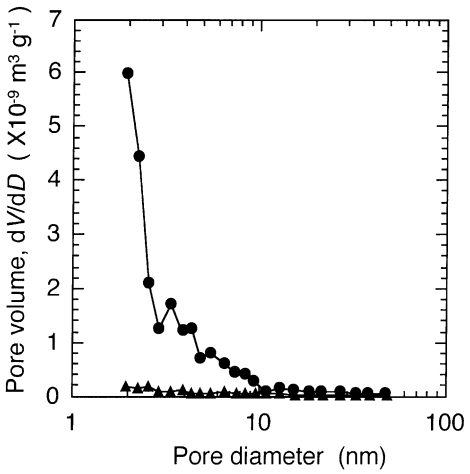

Fig. 8. Pore volume distribution of carbonized paper/pyrolytic carbon sample (▲) and carbonized paper/TiN/pyrolytic carbon sample (●). Number of pulses in PCVI for pyrolytic carbon, 5000.

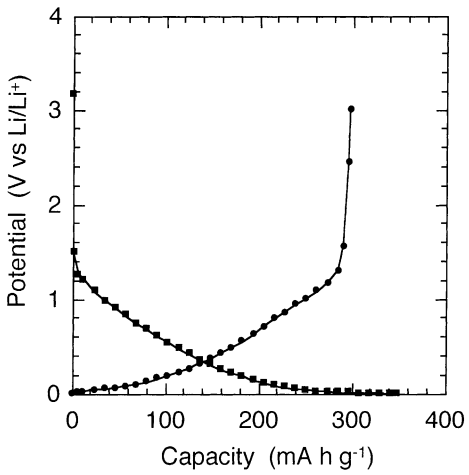

Fig. 9. First charge–discharge curves of carbonized paper/pyrolytic carbon sample obtained after 7000 pulses in PCVI treatment. Current density, 0.2 mA cm^{-2} (12 mA g^{-1}). Capacity was calculated using total mass of the sample.

3.3. Electrochemical properties of carbonized paper/pyrocarbon and carbonized paper/TiN/pyrocarbon samples

Charge–discharge behavior was examined for the samples as-infiltrated by 7000 pulses. Fig. 9 shows the first charge–discharge curves of the carbonized paper/pyrocarbon sample (A). It can be seen that the potential gradually decreases and increases with lithium intercalation and de-intercalation, respectively. The charge–discharge profiles are similar to that usually observed for low crystalline carbon materials having the laminar microstructure (i.e. soft carbon). From the SEM image and XRD pattern of the sample (A) shown in Figs. 4 and 5, respectively, the structure of deposited pyrocarbon is considered to be similar to that of soft carbons. It is supposed that a sloping profile over a range of potentials reflects the crystallinity of pyrocarbon in sample (A), although the sample (A) contains 50 wt.% of the carbonized fibers having the disordered structure. As shown in Fig. 9, the charge capacity on lithium de-intercalation process is 298 mA h g^{-1} per total weight of sample (A). The original carbonized form showed the capacity of 280–320 mA h g^{-1}. The capacity of pyrocarbon in sample (A) seems in the similar range, assuming additivity in capacity. The first Coulombic efficiency for sample (A) is 85%, which is higher than that of the original form (68%). In sample (A), the dense pyrocarbon film with higher crystallinity is coated on the almost all surface of porous carbonized fiber having the disordered structure. In addition, the pyrocarbon film has the laminar texture oriented parallel to the surface of the fiber. It is suggested that the reactive sites (e.g. the crystal edges and the functional groups) at the surface of the carbonized fiber are covered, and the basal planes with low reactivity are mainly exposed to the surface of pyrocarbon-coated fibers in sample (A). These surface structures would reduce the irreversible

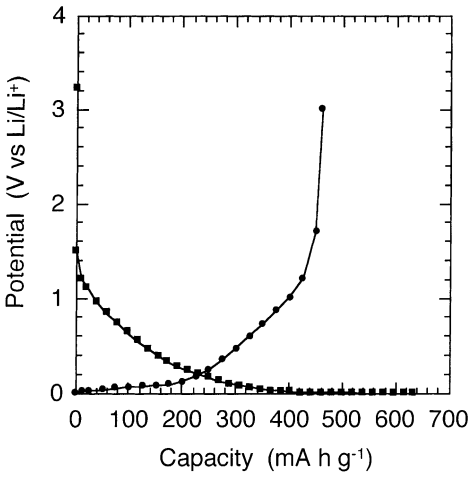

Fig. 10. First charge–discharge curves of carbonized paper/TiN/pyrolytic carbon sample obtained after 7000 pulses in PCVI treatment. Current density, 0.2 mA cm^{-2} (25 mA g^{-1}). Capacity was calculated using the mass of pyrolytic carbon in the sample.

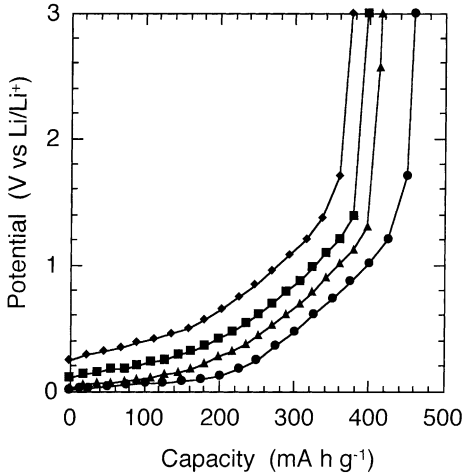

Fig. 11. Charge curves of carbonized paper/TiN/pyrolytic carbon sample at several current density; (●) 0.2 mA cm^{-2} (25 mA g^{-1}), (▲) 0.8 mA cm^{-2} (100 mA g^{-1}), (■) 3.2 mA cm^{-2} (400 mA g^{-1}) and (◆) 8 mA cm^{-2} (1000 mA g^{-1}). Capacity was calculated using the mass of pyrolytic carbon in the sample. Number of pulses in PCVI for pyrolytic carbon, 7000.

reaction such as the decomposition of electrolytes, resulting in high Coulombic efficiency at the first cycle.

Fig. 10 shows the first charge–discharge curves of the carbonized paper/TiN/pyrocarbon sample (B), where the capacity is calculated using only the weight of pyrocarbon in sample (B), considering the significantly low capacity below 10 mA h g^{-1} of the TiN-coated paper form. On the discharge reaction (i.e. lithium intercalation), the potential gradually decreases up to 0.1 V, below which the long plateau appears. In the case of the charging process, the plateau is also observed at the potential below 0.2 V. This behavior is similar to that observed in some non-graphitizing carbon having the disordered structure. As shown in Fig. 9, no low voltage plateau is observed on the discharge or charge curve of sample (A). It have been also reported that the electrochemical properties of pyrocarbon films by CVD were similar to that of the soft carbons [17,19]. From the results of XRD pattern and Raman spectra, it is suggested that the degree of structural disordering in pyrocarbon deposited on TiN-coated fiber {sample (B)} is high in comparison with pyrocarbon deposited directly on carbonized fiber {sample (A)}. The plateau of low voltage would be attributed to the disordering structure of pyrocarbon in sample (B). The charge capacity is 460 mA h g^{-1} per pyrocarbon weight in sample (B). This value is larger than the theoretical capacity of graphite (372 mA h g^{-1}), corresponding to the stage 1 lithium-intercalated graphite, LiC_6. It is supposed that excess lithium is stored in the nano-sized pores in the pyrocarbon of sample (B). 92% of the initial charge capacity was maintained until 60th cycle.

Fig. 11 shows the charge curves of pyrocarbon in sample (B) under different current densities. The capacity at 1000 mA g^{-1} is 80% of that at 25 mA g^{-1}. It is supposed that the relatively high capacity at high charge rate results from the formation of three-dimensional current paths in the active material layers and the tight adhesion between pyrocarbon and TiN, which would be effective in reducing the internal resistance.

Thus, the pyrocarbon deposited on TiN-coated fiber in sample (B) shows the larger capacity than graphite, however, the capacity per total electrode mass becomes lower because of the significantly low capacity of TiN-coated paper fiber used as the conductive filler and/or the current corrector. Fig. 12 shows the charge capacities per total sample mass and the Coulombic efficiencies for both samples (A) and (B). As the mass fraction of pyrocarbon in sample (B) is 26%, the capacity per total mass of sample (B) decreases to around 120 mA h g^{-1}, which is approximately one-fourth of the capacity of pyrocarbon in sample (B). On the other hand, the charge capacity is 298 mA h g^{-1} per total mass of carbonized paper/pyrocarbon sample (A). It is considered that the carbonized fiber form in sample (A) could act not only as the conductive filler and/or current collector but also as the host material for lithium intercalation/de-intercalation, whereas thick TiN film prevents the intercalation of lithium into the carbonized fiber for sample (B). From Fig. 12b, it is found that the first Coulombic efficiency of sample (A) is 85%, which is higher than 72% in sample (B). As mentioned in the previous section, the degree of structural disordering of pyrocarbon in sample (B) is high in comparison with pyrocarbon in sample (A), and BET surface area of sample (B) is also higher than that of sample (A). These structural features of pyrocarbon in sample (B) would cause the increase of irreversible reaction such as the decomposition of electrolytes, resulting in the low Coulombic efficiency at the first cycle. In order to achieve the high capacity per total mass of electrode and Coulombic efficiency for the sample (B), it is necessary to control the thickness of TiN film and to modify the surface of pyrocarbon having the disordered structure.

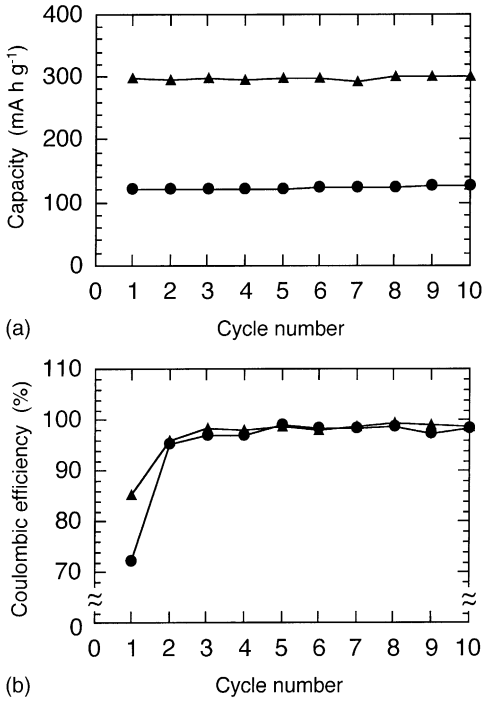

Fig. 12. Charge capacities per total sample mass (a) and Coulombic efficiencies (b) for carbonized paper/pyrolytic carbon sample (▲) and carbonized paper/TiN/pyrolytic carbon sample (●) as a function of cycle number in charge–discharge tests. Number of pulses in PCVI for pyrolytic carbon, 7000.

4. Conclusion

A novel preparation process of negative electrode for lithium-ion rechargeable battery was investigated, consisting of the gas-phase infiltration of pyrocarbon into the electro-conductive porous forms as the conductive fillers and/or current collectors. Using two sorts of conductive porous forms, that is, the carbonized paper (A) and the TiN-coated paper (B), the relation between structure and electrochemical behavior was investigated. The following results have been obtained:

1. The pyrocarbon deposited directly on the carbonized fiber {sample (A)} had the relatively high crystallinity and the laminar texture oriented parallel to the surface of carbonized fiber in paper form. In the pyrocarbon deposited on the TiN-coated fiber {sample (B)}, the degree of structural disordering was high compared with pyrocarbon of sample (A). Sample (B) had higher surface area and larger pore volume with the mesopores of 1.5–10 nm, especially below 3 nm, than sample (A).
2. Sample (B) showed the capacity of 460 mA h g^{-1} per mass of pyrocarbon at a current density of 25 mA g^{-1}. The capacity at 1000 mA g^{-1} corresponded to 80% of that at 25 mA g^{-1}, which would be attributed to the formation of three-dimensionally continuous current paths in the anode-material layer and the tight adhesion between pyrocarbon and TiN to reduce the internal resistance. Thus, the pyrocarbon in sample (B) had the large capacity exceeding the theoretical value of graphite (372 mA h g^{-1}), however, the capacity per total electrode mass was reduced, due to a small capacity of TiN-coated paper fiber used as the conductive filler and/or the current corrector.
3. The capacity of pyrocarbon in sample (A) was estimated at ∼300 mA h g^{-1}, which was lower than that of sample (B). However, the capacity per total electrode mass showed higher value because the carbonized fiber form in sample (A) could act as not only the conductive filler but also the host material for lithium intercalation/de-intercalation. Sample (A) showed higher Coulombic efficiency at first cycle (i.e. 85%), than that of sample (B) (i.e. 72%), which would result from the high crystallinity, the laminar microstructure and the low surface area of pyrocarbon in sample (A).

Acknowledgements

The present work was partly supported by a grant of the Frontier Research project “Materials for the 21st Century—Materials Development for Environment, Energy and Information” (for 2002–2006 fiscal years) from Ministry of Education, Culture, Sports, Science and Technology.

References

[1] S. Ahn, Electrochem. Solid State Lett. 1 (1998) 111.
[2] K. Nishimura, Y.A. Kim, T. Matushita, M. Endo, J. Mater. Res. 15 (2000) 1303.
[3] F. Cheristin, R. Naslain, C. Bernar, in: T.O. Sedgwick, H. Lyoltin (Eds.), Proceedings of the 5th International Conference CVD, Electrochemical Society, New Jersey, 1979, p. 499.
[4] I. Golecki, in: T.M. Besmann, M.D. Allendorf, Mc.D. Robinson, R.K. Ulrich (Eds.), Proceedings of the 13th International Conference CVD, Electrochemical Society, New Jersey, 1996, p. 547.
[5] R. Naslain, J. Alloy Compd. 188 (1992) 42.
[6] O.P.S. Dugne, A. Guette, R. Naslain, R. Fourmeaux, Y. Khin, J. Sevely, J.P. Rocher, J. Cotteret, J. Mater. Sci. 28 (1993) 3409.
[7] T.M. Besmann, R.A. Lowden, B.W. Sheldon, D.P. Stinton, in: K.E. Spear, G.W. Cullen (Eds.), Proceedings of the 11th International Conference CVD, Electrochemical Society, New Jersey, 1990, p. 482.
[8] T.M. Besmann, J.C. Mclaughlin, H.T. Lin, J. Nucl. Mater. 219 (1995) 31.
[9] K. Sugiyama, T. Nakamura, J. Mater. Sci. Lett. 6 (1987) 331.
[10] F. Langlais, P. Dupel, R. Pailler, in: T.M. Besmann, M.D. Allendorf, Mc.D. Robinson, R.K. Ulrich (Eds.), Proceedings of the 13th International Conference CVD, Electrochemical Society, New Jersey, 1996, p. 555.
[11] H.J. Jeong, H.D. Park, J.D. Lee, J.O. Park, Carbon 34 (1996) 417.
[12] Y. Ohzawa, K. Nakane, K. Watabe, K. Sugiyama, Mater. Sci. Eng. B 45 (1997) 114.
[13] K. Sugiyama, Y. Ohzawa, J. Mater. Sci. 24 (1989) 3756.
[14] J.Y. Ofori, S.V. Sotirchos, J. Mater. Res. 11 (1996) 2541.
[15] Y. Ohzawa, K. Nomura, K. Sugiyama, Mater. Sci. Eng. A 225 (1998) 33.
[16] Y. Ohzawa, T. Sakurai, K. Sugiyama, J. Mater. Proc. Tech. 96 (1999) 151.

[17] M. Mohri, N. Yanagisawa, Y. Tajima, H. Tanaka, T. Mitate, S. Nakajima, M. Yoshida, Y. Yoshimoto, T. Suzuki, H. Wada, J. Power Sources 26 (1989) 545.
[18] Y.S. Han, J.S. Yu, G.S. Park, J.Y. Lee, J. Electrochem. Soc. 146 (1999) 3999.
[19] T. Nakajima, M. Koh, M. Takashima, Electrochim. Acta 43 (1998) 883.
[20] M. Ishikawa, M. Morita, T. Hanada, Y. Matsuda, M. Kawaguchi, Denki Kagaku (Electrochem.) 61 (1993) 1395.
[21] A.M. Wilson, J.R. Dahn, J. Electrochem. Soc. 142 (1995) 326.
[22] M.L. Lieberman, in: F.A. Glaski (Ed.), Proceedings of the 3rd International Conference CVD, American Nuclear Society, Utah, 1972, p. 95.
[23] M. Yadasaka, R. Kikuchi, T. Matsui, K. Tasaka, Y. Ohki, S. Yoshimura, E. Ota, J. Vac. Sci. Technol. A 13 (1995) 2142.
[24] M. Yoshio, S. Ozawa, Lithium-ion secondary battery 2, Nikkan Kogyo Shinbun, Tokyo, 2000 (in Japanese).
[25] A. Yoshino, Technical Innovations and Future Prospects on Lithium Secondary battery, NTS, Tokyo, 2001 (in Japanese).
[26] F. Tunistra, J.L. Koenig, J. Chem. Phys. 53 (1970) 1126.
[27] D.S. Night, W.B. White, J. Mater. Res. 4 (1989) 385.